

A meta-analysis of water vapor deuterium-excess in the midlatitude atmospheric surface layer

Lisa R. Welp,¹ Xuhui Lee,^{2,3} Timothy J. Griffis,⁴ Xue-Fa Wen,⁵ Wei Xiao,² Shenggong Li,⁵ Xiaomin Sun,⁵ Zhongmin Hu,⁵ Maria Val Martin,⁶ and Jianping Huang^{2,7}

Received 7 November 2011; revised 20 June 2012; accepted 22 July 2012; published 1 September 2012.

[1] Deuterium-excess (d) in water is a combination of the oxygen ($\delta^{18}\text{O}$) and hydrogen (δD) isotope ratios, and its variability is thought to indicate the location and environmental conditions of the marine moisture source. In this study, we analyze d of water vapor (d_v) from six sites, all between 37 and 44°N to examine patterns in the atmospheric surface layer and identify the main drivers of variability. Two sites are in urban settings (New Haven, CT, USA and Beijing, China), two sites are in agricultural settings (Rosemount, MN, USA and Luancheng, China), and two sites are in natural ecosystems, a forest (Borden Forest, Ontario, Canada) and a grassland (Duolun, China). We found a robust diurnal cycle in d_v at all sites with maximum values during mid-day. Isotopic land surface model simulations suggest that plant transpiration is one mechanism underlying the diurnal pattern. An isotopic large-eddy simulation model shows that entrainment of the free atmosphere into the boundary layer can also produce high d_v values in mid-day. Daily mid-day means of d_v were negatively correlated with local mid-day relative humidity and positively correlated with planetary boundary layer height at the North American sites, but not the Chinese sites. The mechanism for these differences is still undetermined. These results demonstrate that within the diurnal time scale, d_v of the surface air at continental locations can be significantly altered by local processes, and is therefore not a conserved tracer of humidity from the marine moisture source region as has previously been assumed.

Citation: Welp, L. R., X. Lee, T. J. Griffis, X.-F. Wen, W. Xiao, S. Li, X. Sun, Z. Hu, M. Val Martin, and J. Huang (2012), A meta-analysis of water vapor deuterium-excess in the midlatitude atmospheric surface layer, *Global Biogeochem. Cycles*, 26, GB3021, doi:10.1029/2011GB004246.

1. Introduction

[2] Water vapor is the most important atmospheric greenhouse gas, contributing to approximately two-thirds

of the Earth's greenhouse effect [Mitchell, 1989; Intergovernmental Panel on Climate Change, 2007]. Large fluxes of moisture into and out of the atmosphere by evapotranspiration and precipitation replace atmospheric water vapor, on average, every ten days according to global model estimates [Trenberth *et al.*, 2007]. As global temperatures increase, it is expected that evapotranspiration will also increase, leading to more water vapor in the atmosphere and a positive feedback on climate forcing. Indeed, there is some evidence that the specific humidity of the atmosphere is already increasing due to anthropogenic influences [Santer *et al.*, 2007; Willett *et al.*, 2007].

[3] Stable isotopes of hydrogen and oxygen in water are useful tracers in the global hydrological cycle [Gat, 1996]. Differences in the rates of evaporation and condensation between heavy and light isotopologues of water create spatial and temporal variability in the isotopic composition of water in the air and also on the land surface (i.e., lakes, rivers, soils, and plants). There are currently efforts to utilize stable isotopes as an additional constraint on water cycling in atmospheric general circulation models [e.g., Henderson-Sellers, 2006; Lee *et al.*, 2007a; Yoshimura *et al.*, 2008; Risi *et al.*, 2010; Werner *et al.*, 2011]. The isotopic composition

¹Scripps Institution of Oceanography, University of California, San Diego, La Jolla, California, USA.

²Yale-NUIST Center on Atmospheric Environment, Nanjing University of Information Science and Technology, Nanjing, China.

³School of Forestry and Environmental Studies, Yale University, New Haven, Connecticut, USA.

⁴Department of Soil, Water, and Climate, University of Minnesota, Twin Cities, St. Paul, Minnesota, USA.

⁵Key Laboratory of Ecosystem Network Observation and Modeling, Institute of Geographic Sciences and Natural Resources Research, Chinese Academy of Sciences, Beijing, China.

⁶Department of Atmospheric Science, Colorado State University, Fort Collins, Colorado, USA.

⁷I. M. System Group, Environmental Modeling Center, NOAA National Centers for Environmental Prediction, Camp Springs, Maryland, USA.

Corresponding author: L. R. Welp, Scripps Institution of Oceanography, University of California, San Diego, 9500 Gilman Dr., La Jolla, CA 92093-0244, USA. (lwelp@ucsd.edu)

of precipitation has been monitored and studied for several decades by the International Atomic Energy Agency Global Network of Isotopes in Precipitation (IAEA GNIP) network [Rozanski *et al.*, 1993]. By comparison, there are relatively few measurements of the isotopic composition of water vapor in the lower troposphere because it required labor-intensive cryogenic trapping [e.g., *Jacob and Sonntag*, 1991; *Gat et al.*, 1994; *He and Smith*, 1999]. Therefore, most of our understanding of isotope hydrology and ecohydrology has come from the condensed or liquid phase [Gat, 1996].

[4] Variability in hydrogen and oxygen isotopes of water is measured as changes in the ratio of heavy to light isotopologues (R): deuterium to hydrogen (D/H) and oxygen mass 18 to mass 16 ($^{18}\text{O}/^{16}\text{O}$). Isotope ratios are commonly reported relative to a standard in delta-notation,

$$\delta = \frac{R_{\text{sample}}}{R_{\text{standard}}} - 1 \quad (1)$$

where the standard used is Vienna Standard Mean Ocean Water (VSMOW) and are multiplied by 1000 to express in parts per thousand (‰) or per mil. *Craig* [1961] observed that the δD and $\delta^{18}\text{O}$ of precipitation worldwide could be fit by a straight line, $\delta\text{D} = 8 \times \delta^{18}\text{O} + 10\text{‰}$, and defined this as the Global Meteoric Water Line (GMWL). The GMWL slope of 8 in $\delta^{18}\text{O}$ - δD space is the result of equilibrium condensation processes and the ratio of equilibrium fractionation factors for D and ^{18}O [Clark and Fritz, 1997]. The GMWL intercept of 10‰ is the result of average equilibrium and kinetic fractionation during evaporation from the ocean with a global evaporation-weighted mean relative humidity of 85% [Clark and Fritz, 1997].

[5] Deuterium-excess (d) defines offsets in δD from the GMWL [Dansgaard, 1964].

$$d = \delta\text{D} - 8 \times \delta^{18}\text{O} \quad (2)$$

Values that fall on the GMWL have a d of 10‰ by definition. Since equilibrium Rayleigh condensation processes roughly follow the GMWL slope of 8, deviations in d can provide information about the environmental conditions during non-equilibrium processes such as relative humidity (h) and temperature in oceanic moisture source regions. That is, d is thought to be a conservative tracer of oceanic evaporation conditions, useful for identifying moisture source locations, if there are no contributions from surface evapotranspiration as the air mass travels over land [Uemura *et al.*, 2008]. Theory predicts that d of evaporating vapor increases as humidity decreases ($-0.43\text{‰}/\%$) and as temperature increases ($0.35\text{‰}/^\circ\text{C}$) [Merlivat and Jouzel, 1979]. There have been a few field measurements in marine-like settings to quantify the humidity and temperature dependencies of d in vapor evaporating from the ocean and Mediterranean Sea using traditional cryotrapping techniques giving a range of values around the theoretical prediction [Gat *et al.*, 2003; Pfahl and Wernli, 2008; Uemura *et al.*, 2008]. Deuterium-excess measured in ice cores has often been used as a proxy to reconstruct paleo-temperature and humidity of oceanic moisture source regions using this theory [e.g., Jouzel *et al.*, 1982; Cuffey and Vimeux, 2001; Masson-Delmotte *et al.*, 2005; Steffensen *et al.*, 2008].

[6] In continental settings, the vapor produced by evaporating meteoric waters, which themselves have d values close to 10‰, in under-saturated conditions tends to have δD and $\delta^{18}\text{O}$ lower than the liquid and d greater than 10‰. Again, this is controlled by the relative humidity of the air at the evaporative surface and temperature of the water [Clark and Fritz, 1997]. Addition of this ‘recycled’ moisture to an air mass either from terrestrial bodies of open water [Gat *et al.*, 1994], or from terrestrial evapotranspiration [Kurita *et al.*, 2004] can change the original vapor d signal from ocean evaporation and may be used to quantify the recycled moisture input from dense networks of precipitation isotope observing sites.

[7] Recent developments in spectroscopic techniques to measure $\delta^{18}\text{O}$ and δD in real time without cryogenic trapping now make it possible to examine variability in hydrogen and oxygen isotopes in water vapor on timescales of an hour or less [e.g., Lee *et al.*, 2005; Wen *et al.*, 2008; Wang *et al.*, 2009; Schmidt *et al.*, 2010; Johnson *et al.*, 2011]. Some of the first publications of high frequency $\delta^{18}\text{O}$ and δD of water vapor show that there is much more variability than originally expected [Lee *et al.*, 2006; Welp *et al.*, 2008; Wen *et al.*, 2010]. It is also possible to retrieve vertical profiles of δD with high spatial coverage from satellite observations, but unfortunately not precise $\delta^{18}\text{O}$ at the moment [e.g., Worden *et al.*, 2006; Schneider and Hase, 2011]. Using satellite measurements, researchers have shown that rain evaporation and surface evapotranspiration significantly contribute to the tropospheric water budget in the tropics [Worden *et al.*, 2007].

[8] Identifying sources of moisture to the atmosphere is relatively complicated because several processes contribute to changes in tropospheric and atmospheric boundary layer vapor δD and $\delta^{18}\text{O}$. These processes include: (i) isotopic fractionation (both equilibrium and kinetic) associated with in-cloud condensation and rainout processes; (ii) turbulent mixing of different air masses with different moisture sources and δ values; (iii) entrainment of free tropospheric air into the boundary layer; (iv) the addition of heavy moisture from surface evapotranspiration; and (v) partial evaporation of raindrops below the cloud base [Stewart, 1975; Darling *et al.*, 2006]. Other influences are confined mainly to the stratosphere: lofting and evaporation of ice crystals, and photooxidation of methane [Johnson *et al.*, 2001].

[9] To date, most water isotope observational studies have focused on a single tracer, either $\delta^{18}\text{O}$ or δD , but it may be possible to leverage d to isolate a few of the processes listed above in some circumstances. For example, cloud condensation and rainout processes governed by Rayleigh distillation are the first-order driver of changes in δD and $\delta^{18}\text{O}$, but have a much smaller effect on d [Gat, 1996]. Several questions still remain as to the dominant processes controlling d_v variability in the boundary layer [Lai and Ehleringer, 2011], but the recent proliferation in vapor isotope measurements allows the usefulness of the d tracer to be examined like never before.

[10] Here, we present d of vapor (d_v) measurements from six midlatitude sites on two continents to compare geographic variability and to investigate the correlations with environmental parameters and atmospheric structure. We examine d_v variability on time scales ranging from monthly to hourly. We also qualitatively evaluate the potential

Table 1. Summary of Site Locations, Characteristics, and Measurement Specifics

	New Haven	Borden	Rosemount	Beijing	Duolun	Luancheng
Vegetation type	Urban	Forest	Corn	Urban	Grassland	Corn/Wheat
Latitude	41°18'N	44°19'N	44°42'N	40°00'N	42°02'N	37°50'N
Longitude	72°55'W	79°56'W	93°05'W	116°23'E	116°17'E	114°40'E
Surface elevation (masl)	9	240	294	45	1324	50
Intake height (magl)	15	37	3.5	10	1.6	4
Start date	27-Mar-07	27-May-09	16-Jun-09	10-Dec-06	1-Jun-09	1-Apr-08
End date	31-May-08	19-Aug-09	2-Sep-09	10-Dec-07	17-Sep-09	14-Sep-08
Data gaps (summer only)	14%	22%	18%	4%	16%	3%
Reference	<i>Lee et al.</i> [2006]	<i>Santos et al.</i> [2011]	<i>Griffis et al.</i> [2011b]	<i>Wen et al.</i> [2010]	<i>Wen et al.</i> [2011]	<i>Wen et al.</i> [2011]

contributions from the following sources: plant transpiration, surface evaporation, vertical mixing and entrainment, and the effect of the nonlinearity of the delta-notation to the robust diurnal variability in d_v seen at all sites during summer months.

2. Site Descriptions

[11] Table 1 provides a summary of the six sites where the vapor isotope measurements were made. The reader is referred to the primary references included in Table 1 for detailed descriptions of these measurement sites. Urban observations were made in Beijing, China and New Haven, CT, USA. Beijing summers are hot and humid as a result of the East Asian summer monsoon influence. The mean annual precipitation is 560 mm, of which approximately 80% occurs during monsoon season (June through September). New Haven summers are also hot and humid as the dominant weather patterns move offshore. The mean annual precipitation is 1340 mm, evenly distributed throughout the year.

[12] Agricultural observations were made at research sites in Luancheng, China and Rosemount, MN, USA. The Luancheng site was a field of wheat and corn (or maize) rotation and the Rosemount site was planted with corn. During the periods of isotope measurements, maximum leaf area index (LAI) was $4.2 \text{ m}^2 \text{ m}^{-2}$ at Luancheng and $6.4 \text{ m}^2 \text{ m}^{-2}$ at Rosemount. The grassland observations were conducted in Duolun County, a semiarid area located in Inner Mongolia, China. The site has been fenced since 2001 as a long-term study plot, and is dominated by C_3 species, e.g., *Stipa kryroii*, *Agropyron cristatum*, and *Artemisia frigida* [Zhang et al., 2007; Xia et al., 2009]. According to our measurements, the three dominant species account for approximately 75% of the total aboveground biomass of the community in the peak growing-season. Maximum LAI was $0.5 \text{ m}^2 \text{ m}^{-2}$. The forest site was located near Borden, Ontario, Canada. The forest was a mixture of aspen and maple trees. The mean LAI during the growing season was $3.8 \text{ m}^2 \text{ m}^{-2}$.

[13] The vapor isotope measurements were analyzed against meteorological data. For New Haven, we obtained air temperature, wind direction, cloud conditions, and precipitation time and amount at the Tweed Airport (41°16'N/72°53'W), approximately 7 km SE from the isotope sampling site, from the U.S. National Weather Service (station ID 065273). For Beijing, these data were obtained with a weather station mounted on the rooftop of the laboratory building near the ambient air intake for isotope

measurements, at 20 m above the ground [Wen et al., 2010]. For the other sites, standard micrometeorological variables were measured at the same location of the vapor sampling and are described in the primary references listed in Table 1.

[14] When discussing similarities and differences among sites, we often found that the sites in northeastern North America behaved similarly and were different from those in northeastern China. For convenience, we sometimes group the sites in our discussion by location. It is not our intent to suggest that these 3 sites per continent represent isotopic conditions on the entire continent.

3. Methods and Data

3.1. Isotope Measurements

[15] We made continuous measurements of the HDO/H₂O and H₂¹⁸O/H₂¹⁶O ratios in water vapor using tunable diode laser (TDL) absorbance spectroscopy (TGA100A and TGA200, Campbell Scientific, Inc., Logan, UT, USA). The sampling setup was similar at all sites and included at least one atmospheric intake above the ground surface, two calibration span gases and one zero that cycled through the TDL for ~25 s each. TDL output was recorded a 1 Hz by a data logger (Model CR1000, Campbell Scientific Inc., Logan, UT, USA). A dynamic calibration system, referred to as the 'dripper', allowed us to correct for instrument nonlinearity in the TDL measurement with respect to absolute water content by adjusting the mixing ratio of the water in our calibration span gases [Lee et al., 2005, 2006; Wen et al., 2008]. The sampling setup at Rosemount was slightly different than the other sites because it was running in eddy covariance mode instead of flux gradient or single atmospheric observation modes [Griffis et al., 2010].

[16] The isotope ratio of atmospheric water vapor (R_v) was averaged over the 25 s sampling interval and calibrated for each cycle according to the method described in Wen et al. [2008]. Gaps in the data during summer months (June through August) ranged from 3% at Luancheng to 22% at Borden (Table 1). The remaining results were averaged together to construct hourly means. The hourly one standard deviation precision was approximately 0.11‰ for $\delta^{18}\text{O}$ and 1.1‰ for δD at a dewpoint temperature of 15°C and 0.12‰ for $\delta^{18}\text{O}$ and 2.0‰ for δD at a dewpoint temperature of 1°C [Wen et al., 2008]. Error propagation results in a precision for d of approximately 2‰.

3.2. Nonlinearity of the Delta-Notation

[17] Rayleigh rainout processes control most of the variability seen in $\delta^{18}\text{O}$ and δD . In fact, those processes are responsible for the observed GMWL, and since d is defined as the offset from the GMWL, Rayleigh signals are greatly suppressed in d values. However, the equations governing Rayleigh fractionation are derived using lambda-notation, $\lambda = \ln(R_{\text{sample}}/R_{\text{standard}})$ and using the delta-notation approximation leads to errors in δD [Gat, 1996]. This means that Rayleigh rainout processes do have the power to change d_v slightly. The slope of the Rayleigh lines in lambda-notation (S_λ) is:

$$S_\lambda = \frac{\epsilon_D^*}{\epsilon_{18}^*} \quad (3)$$

where ϵ_D^* and ϵ_{18}^* are the equilibrium fractionation factors for D/H and $^{18}\text{O}/^{16}\text{O}$ respectively. It is this ratio of the fractionation factors that results in Rayleigh slopes near 8 at temperatures in the range of 0–30°C. Plotting Rayleigh lines in $\delta^{18}\text{O} - \delta\text{D}$ (‰) space and calculating d using delta-notation introduces a deviation from linearity that becomes larger as the δ values become further removed from zero [Gat, 1996]. The slope of the Rayleigh lines in delta-notation (S_δ) is:

$$S_\delta = \frac{\epsilon_D^* \cdot (1 + \delta_v^{\text{D}}/10^3)}{\epsilon_{18}^* \cdot (1 + \delta_v^{18}/10^3)} \quad (4)$$

The correction terms $(1 + \delta_v/10^3)$ become significant as vapor δ values become large negative numbers, particularly in the case of δD . Therefore, even when Rayleigh theory is perfectly followed, large decreases in vapor $\delta^{18}\text{O}$ and δD , as during times of low water vapor mixing ratios [Lee *et al.*, 2006; Wen *et al.*, 2010], cause a slight increase in d due to the nonlinearity of the delta-notation.

3.3. PBL Heights

[18] Planetary boundary layer (PBL) mixing height was obtained from the NASA GEOS-5 Modern Era Retrospective-Analysis for Research and Applications (MERRA) meteorological fields [Jordan *et al.*, 2010]. The GEOS-5 MERRA fields had a 0.5° latitude by 0.67° longitude horizontal resolution and one-hour temporal resolution. PBL heights were extracted at the location of the sites. Precise estimates of PBL height become difficult during cloudy and stormy conditions. We excluded periods of rain from our analysis, but retained cloudy conditions with no precipitation.

3.4. Isotope Models

[19] We used two isotope models to probe the mechanisms underlying the observed diurnal variation in d_v . The isotopic large-eddy simulation model (ISOLES) of Lee *et al.* [2012] was used to simulate the entrainment influence on d_v . The isotopic land surface model (IsoLSM) of Xiao *et al.* [2010] was used to simulate the diurnal changes in the d of the transpiration flux at Luancheng.

4. Results and Discussion

4.1. Monthly and Synoptic Variability

[20] All of the vapor isotope measurements from each site are plotted in $\delta^{18}\text{O}$ - δD space in Figure 1. In each case, the

$\delta^{18}\text{O}$ and δD data cluster around the GMWL, with higher summer values showing a tighter fit to the GMWL than lower winter values. The large scatter around the GMWL at Rosemount may be because this was the only site that did not use a buffer volume on the ambient intake sampling line to dampen short-term variability.

[21] The New Haven and Beijing sites had the longest duration of continuous measurements of about a year, making it possible to examine the seasonal variability of d in vapor and precipitation. Figure 2 shows the monthly arithmetic mean d_v and the amount-weighted precipitation d . At both sites, d_v was usually greater than precipitation d . In general, both vapor and precipitation d were lowest during summer months. This is in contrast to the seasonal cycles in $\delta^{18}\text{O}$ and δD , which have summer maximums. Summer minima in d_v was previously observed by Jacob and Sonntag [1991] over eight years in Heidelberg, Germany and by Angert *et al.* [2008] over nine years in Rehovot, Israel. The mean seasonal cycle of d in northern hemisphere precipitation from the IAEA GNIP database is also at a minimum in the summer months [Araguas-Araguas *et al.*, 2000]. Angert *et al.* [2008] describe how the seasonal variability in d_v in Israel can be explained by changes in the initial vapor from the Mediterranean Sea superimposed on Rayleigh isotopic distillation. Initial vapor is modified by monthly variability in temperature and relative humidity near the surface of the Mediterranean Sea and varying rates of moisture entrainment from the lower troposphere into the PBL.

[22] In Beijing, monthly variability in d_v has a negative linear correlation with temperature ($p = 0.001$, slope = $-0.46\text{‰ per }^\circ\text{C}$), water vapor mixing ratio ($p = 0.002$, slope = $-0.52\text{‰ per mmol mol}^{-1}$), but not well correlated with precipitation amount ($p = 0.10$) or relative humidity ($p = 0.24$). In New Haven, monthly variability in d_v is not well correlated with any of these environmental variables ($p > 0.20$ in all cases).

[23] Mean summer d_v at the North American sites were higher than at the Chinese sites by approximately 7‰ (Table S1 in the auxiliary material) even though they are all at nearly the same latitude.¹ This general pattern is predicted from a model interpolation of the IAEA GNIP database, showing high values of d of precipitation downwind of the Great Lakes [Bowen and Revenaugh, 2003]. Evaporation from the Great Lakes is expected to have higher d values than the air masses transported to this region. Gat *et al.* [1994] used high d in precipitation from the Northeastern U.S., presumably resulting from d_v anomalies, to estimate that recycled continental moisture from evaporation off the Great Lakes contributed 4–16% of precipitation downwind of the lakes in the summer.

[24] We also observed differences in the synoptic variability in the concurrent measurements at New Haven and Beijing (Figure 3). The 10-day running means were more variable at New Haven than at Beijing. New Haven is located in the northeast of U.S. where all the major storm tracks converge and experiences weather cycles every 7–10 days throughout the year [Zielinski and Keim, 2003] bringing with them moisture from different source regions. In comparison,

¹Auxiliary materials are available in the HTML. doi:10.1029/2011GB004246.

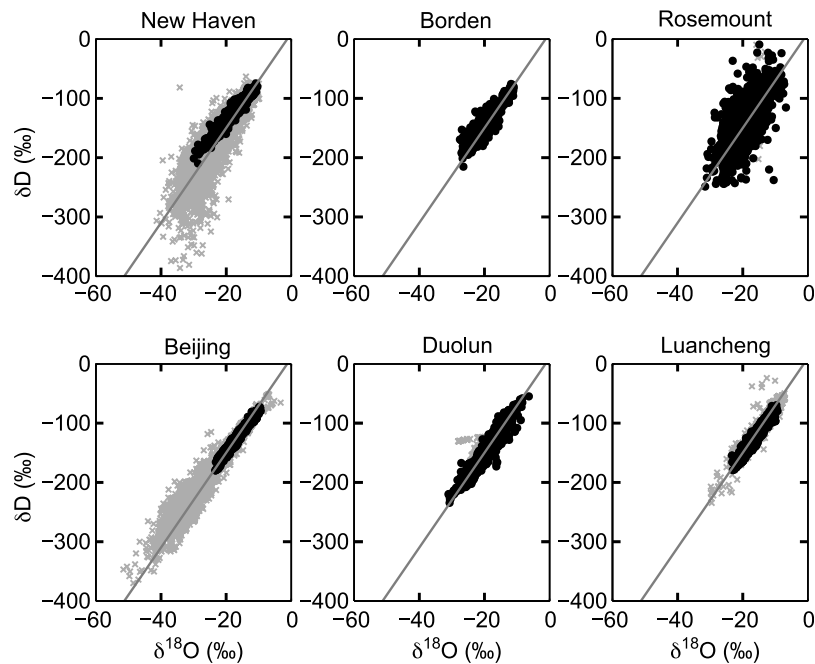


Figure 1. Vapor measurements of δD and $\delta^{18}O$ at each site, over the entire period of measurement (light gray crosses) and for June–August (black circles). For reference, the GMWL is plotted with each site (dark gray line). Deuterium-excess (d) is a measure of the deviation from the GMWL in δD (‰).

frontal activities are less frequent in Northeast China in the warm season. *Wen et al.* [2010] proposed that the Asian monsoon suppresses variability in d_v in the summer by maintaining a relatively consistent moisture source region.

4.2. Day-to-Day Variability

[25] If d_v is a conservative tracer of conditions in the moisture source region, we would not expect it to vary with local h unless there is a local source of moisture to the atmosphere. Afternoon averages (12:00–18:00 local standard time) of d_v were correlated with h at New Haven ($d_v/h = -0.36\text{‰}/\%$, $r = -0.74$, $p < 0.001$) and Borden Forest ($d_v/h = -0.22\text{‰}/\%$, $r = -0.57$, $p < 0.001$) sites during the summer months (June–August), suggesting that local contributions of moisture are relatively high (Figure 4 and Table 2). The afternoon period was chosen because correlations during this time were the higher than any other time of day or the daily mean. This is also the time of the day when the surface measurements are most representative of regional conditions due to increased atmospheric turbulence. These two particular sites are located near large bodies of water, which may contribute significant amounts of moisture to the sites. New Haven sits on Long Island Sound adjacent to the Atlantic Ocean. Located between Lake Huron and Lake Ontario, Borden Forest is approximately 20 km southeast of the Georgian Bay. Although we did not observe significant linear correlations between d_v and h afternoon averages at Beijing and Luancheng during the summer, *Wen et al.* [2010] reports weak nonlinear correlations between hourly d_v and local h at these sites outside periods of peak summer monsoon activity from the same data set. That Borden and New Haven show significant correlations, whereas the more inland sites do not, suggests that a stronger correlation may be indicative of a higher contribution of local water sources

to the atmospheric moisture. The footprint of the source influence appears to have extended tens of kilometers beyond the local site scale, even though the measurements were made near the ground.

[26] The variability in d_v/h relation in marine-type settings in the literature ranges from -0.31 to -0.61‰ per $\%$ for vapor evaporated from the Mediterranean Sea and southern ocean [*Gat et al.*, 2003; *Pfahl and Wernli*, 2008; *Uemura et al.*, 2008]. The New Haven slope (-0.36) is within the range of ocean/sea vapor observations from the literature, but the Borden Forest slope (-0.22) is lower. To our knowledge, this is the first terrestrial observation showing a relation between d_v and h . A possible explanation for the lower observed d_v/h slope at Borden Forest, compared to literature values, is that they calculate h relative to the sea surface temperature at or near the site of evaporation, whereas our comparison used h calculated relative to air temperature at the vapor measurement site downstream of the suspected moisture source. However, our attempt to correct measured h relative to NOAA buoy water temperature or air temperature just above the water surface of the assumed moisture source regions (Long Island Sound in the case of New Haven and Lake Ontario in the case of Borden Forest) revealed lower d_v/h slopes (Table S2 in the auxiliary material).

[27] It is well known that water vapor mixing ratio controls much of the variability in $\delta^{18}O$ and δD [*Lee et al.*, 2006; *Wen et al.*, 2010] due to Rayleigh distillation processes. It is not expected that this would extend to d_v as well because Rayleigh distillation should not greatly affect d_v , with the exception of the nonlinearity effects described in the Methods section. We found that afternoon averages of d_v were strongly negatively correlated with water vapor mixing ratio at all sites except Beijing (Table 2 and Figure S1 in the auxiliary material, $p < 0.001$). Similar to the case of the

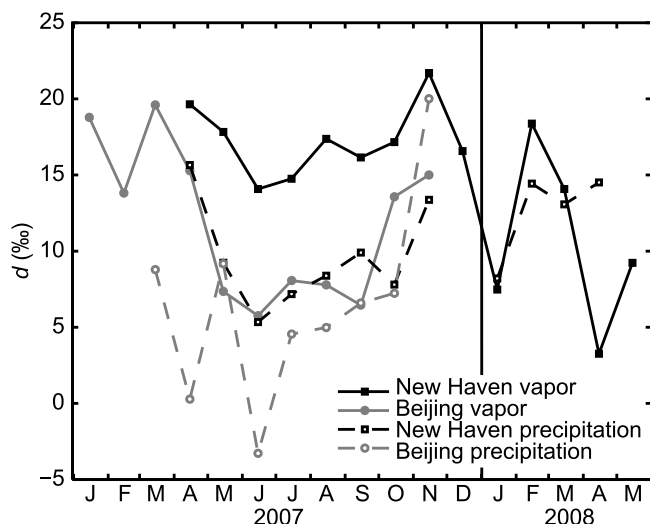


Figure 2. Monthly arithmetic mean of vapor d (solid lines) and amount-weighted precipitation d (dashed lines) for the New Haven (black) and Beijing (gray), January 2007 through May 2008.

correlation with h , changes in water vapor mixing ratio appear to have a larger effect on d_v (i.e., higher slopes) at the North American sites than at the Chinese sites. It could be that water vapor mixing ratio is also a good predictor of d_v at least at some sites, but the mechanism causing such a relationship is difficult to identify at this point. None of the sites showed a significant correlation between d_v and local air temperature (Table 2).

4.3. Diurnal Variability

[28] Figure 5a shows the mean diurnal cycles of d_v from each site during the summer months (June–August). This three-month period was selected because measurements were made at all sites during these months, and they represent the growing season at midlatitudes in the northern hemisphere. We found that d_v varied diurnally, showing a clear, robust pattern of maximum d_v during the afternoon at all sites. This extends the finding of *Wen et al.* [2010], which previously published the results from the Beijing site, and it is consistent with the observations of *Lai and Ehleringer* [2011] over a few days in the Pacific Northwest. The study presented here is the most extensive set of continuous measurements of diurnal variability in d_v to date and shows that daytime d_v increase is not a pattern unique to any one location or vegetation type. The nighttime ‘baseline’ values of the Chinese sites are approximately 6‰ lower than the North American sites, similar to the offset in summer mean values already discussed.

[29] The phases are remarkably similar despite widely varying local vegetation types. The site that is most different from the others in terms of amplitude and phase is Beijing. It is also the most densely populated urban environment with large amounts of impermeable surfaces, and the influence of transpiration should be negligible and evaporation should be small at this site. In contrast, New Haven, the other urban site, has a large fraction of tree vegetation cover (49%, <http://nrs.fs.fed.us/data/urban/>) and is located in close proximity to

the Atlantic Ocean, resulting in higher transpiration and evaporation influence.

[30] Although the phases are similar at all sites, the peak-to-trough amplitudes vary greatly: 3.5‰ at Beijing, 7.7‰ at Luancheng, 9.8‰ at New Haven, 10.0‰ at Borden Forest, 13.5‰ at Duolun, and 17.1‰ at Rosemount (Figure 5a). Note that the Rosemount amplitude may be overestimated in this analysis because of the large amount of noise in the data. Clearly within the diurnal time scale, d_v is not a conserved tracer of humidity conditions at the marine moisture source region. For example, a diurnal amplitude of 9.8‰ at New Haven would imply an uncertainty of 27% in the inferred relative humidity at the source.

[31] We find that the mid-day decrease in $\delta^{18}\text{O}$ of water vapor, combined with little to no change in δD , leads to the variability in d_v (Figures 5b and 5c). Several previous studies have examined controls of the diurnal variability of $\delta^{18}\text{O}$ of water vapor, and it is likely that some of the same processes may explain the variability in d_v . The morning decrease in $\delta^{18}\text{O}$ has been attributed to the rapid increase of air entrained into the boundary layer during convective mixing [*Lai et al.*, 2006; *Welp et al.*, 2008; *Zhang et al.*, 2011]. Later in the day, the increase in $\delta^{18}\text{O}$ may be driven by surface evapotranspiration, because evapotranspiration acts to enrich the surface vapor in ^{18}O [*Lee et al.*, 2012]. *Lai and Ehleringer* [2011] is one of the few studies that investigated the diurnal variability in d_v , and they also conclude that entrainment and evapotranspiration play dominant roles in d_v variability in the early morning and late afternoon, respectively.

[32] The nonlinearity of the delta-notation definition may contribute to the increased d_v during mid-day (see comment on the approximation of the delta-notation in the Methods section). This effect was taken into account recently in the seasonal cycle of d_v in *Angert et al.* [2008]. We estimate that the nonlinearity of the delta-notation contributes to $\sim 10\%$ or less of the diurnal amplitude in d_v . Because the daily minimum of $\delta^{18}\text{O}$ and δD are not at the same time, the nonlinearity errors are either positive or negative at different sites, ranging from -1.6 to 0.4% (Table S3 in the auxiliary

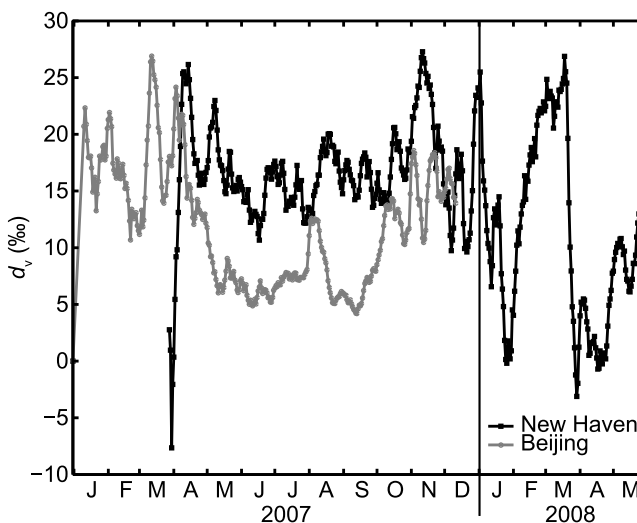


Figure 3. Ten-day running mean of d_v from Jan 1, 2007 to May 31, 2008 at New Haven (black) and Beijing (gray).

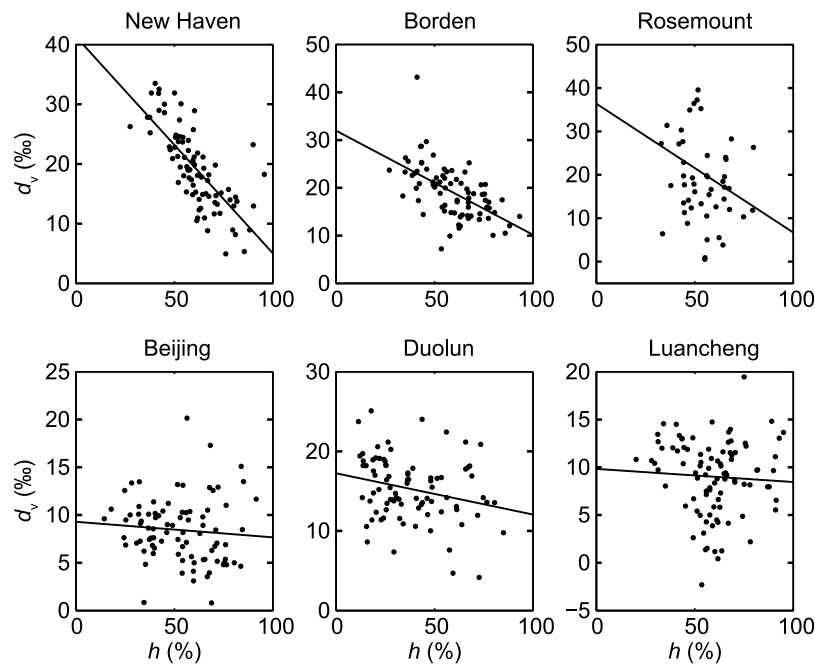


Figure 4. Afternoon (12:00–18:00 local time) mean d_v versus afternoon mean h in the summer (June–August). Only New Haven and Borden sites have significant negative correlations. Changing the averaging time window within the daytime period does not affect the correlation pattern across sites. Fit statistics are summarized in Table 2.

material). We conclude that this effect is not a significant contributor to the diurnal cycle of d_v at the sites we observed.

[33] To examine entrainment, which has been identified as a major contributor to the diurnal cycle of vapor isotopes from other studies, we compared afternoon mean vapor isotopes at each site with modeled estimates of the PBL height (Figure 6 and Table 2). Although the PBL height is controlled by several factors, it has been shown that the entrainment of free tropospheric air is the leading order control providing the energy to grow the PBL [Medeiros *et al.*, 2005], and we use it here as a rough proxy for entrainment. Afternoon d_v was significantly correlated with PBL height at New Haven (slope = 8.5‰/km, $p < 0.001$) and Borden Forest (slope = 8.7‰/km, $p < 0.001$). On days with higher PBL heights, d_v was higher at these sites. Rosemount also showed a similar slope, but with less statistical significance (slope = 8.6‰/km, $p = 0.021$). This site also has a higher degree of noise in the data, which could reduce the correlation significance. Correlations were not significant at the Chinese sites ($p > 0.13$).

[34] Interestingly, afternoon PBL height correlations with $\delta^{18}\text{O}$ were the largest and most significant at the North American sites (slopes range from -2.9 to -4.9‰ km^{-1} , $p < 0.003$) as were the correlations with afternoon δD (slopes range from -14.5 to -30.6‰ km^{-1} , $p < 0.03$) (Table 2). These results suggest that the isotope ratios of water vapor could vary more with height in the atmosphere in some areas like northeastern North America, than others, like near Beijing, China.

[35] An increase in d_v with height in the atmosphere could explain our observations at the North American sites. To our knowledge, there is limited evidence of d_v increasing with height in the lower troposphere. Griffis *et al.* [2011a]

showed that d_v measured in Rosemount was, on average, 5.1‰ greater at 200 m than at 3 m, from measurements made including the cold season, starting April 2010 through June 2011, and that the difference approaches zero during periods of strong daytime mixing. Measurements made near New Haven by He and Smith [1999] showed that the free atmosphere d_v was $\sim 8\text{‰}$ higher than the atmospheric boundary layer value. There is also evidence of extremely large d_v values in the upper troposphere and lower stratosphere of the tropics and subtropics [Webster and Heymsfield, 2003]. While our analysis suggests that entrained air has higher d_v than the surface, Lai and Ehleringer [2011] predicted that air entrainment exerted a negative isotope forcing in the early morning on their three study days in the Pacific Northwest and switched to a positive isotope forcing on the afternoons of the last two days. It should be noted that they used measurements of d_v at 60 m to estimate the isotopic composition of the entrained air. While the addition of surface moisture via evapotranspiration may be able to explain vertical profiles of $\delta^{18}\text{O}$ and δD , it has the wrong sign in the case of d_v , adding higher values of d_v near the surface.

[36] In the interpretation of Figure 6, we assume that a higher PBL height in mid-afternoon is associated with faster PBL growth and therefore a stronger entrainment rate. If there is a vertical gradient in d_v increasing with height, entrainment could easily explain the diurnal cycle in d_v . To support this argument, we parameterized the ISOLES model with typical midlatitude summer conditions. In the model domain, the evolution of the PBL was forced by a time-varying solar radiation, a prescribed initial specific humidity profile in the early morning [Lee *et al.*, 2012] and initial profiles of $\delta^{18}\text{O}$ and δD according to the observed

Table 2. Linear Least Squares Fits Between Afternoon Means (12:00–18:00) During June–August, Correlations and Statistics^a

Site	m	b	sm	sb	R	P
<i>d_v (%) Versus h (%)</i>						
New Haven	-0.36	41.35	0.04	2.30	-0.74	<0.001
Borden	-0.22	31.96	0.04	2.21	-0.57	<0.001
Rosemount	-0.30	36.38	0.19	10.52	-0.22	0.125
Beijing	-0.02	9.30	0.02	1.13	-0.09	0.424
Duolun	-0.05	17.24	0.02	0.95	-0.25	0.022
Luancheng	-0.01	9.83	0.03	1.56	-0.06	0.584
<i>d_v (%) Versus Temperature (°C)</i>						
New Haven	-0.01	19.61	0.21	5.10	-0.01	0.949
Borden	-0.15	22.48	0.16	3.56	-0.11	0.339
Rosemount	-0.99	43.43	0.51	12.12	-0.23	0.056
Beijing	0.19	2.63	0.12	3.64	0.17	0.110
Duolun	-0.07	16.79	0.10	2.34	-0.07	0.506
Luancheng	-0.18	14.23	0.11	3.06	-0.18	0.088
<i>d_v (%) Versus H₂O (mmol/mol)</i>						
New Haven	-0.94	36.87	0.11	2.03	-0.70	<0.001
Borden	-0.85	32.44	0.11	1.75	-0.67	<0.001
Rosemount	-1.85	52.09	0.31	5.75	-0.57	<0.001
Beijing	-0.02	8.95	0.07	1.46	-0.04	0.738
Duolun	-0.40	19.96	0.09	1.15	-0.43	<0.001
Luancheng	-0.25	15.15	0.08	2.01	-0.31	0.002
<i>d_v (%) Versus PBL Height (km)</i>						
New Haven	8.50	9.02	1.25	1.62	0.60	<0.001
Borden	8.70	9.91	1.81	1.99	0.48	<0.001
Rosemount	8.64	5.72	3.68	5.87	0.27	0.021
Beijing	-0.67	9.44	0.66	1.01	-0.11	0.308
Duolun	1.32	12.85	0.85	1.61	0.17	0.125
Luancheng	-0.06	9.09	0.73	1.09	-0.01	0.930
<i>h (%) Versus PBL Height (km)</i>						
New Haven	-22.70	88.77	2.00	2.59	-0.77	<0.001
Borden	-30.04	90.66	4.02	4.48	-0.65	<0.001
Rosemount	-15.48	78.57	2.94	4.79	-0.60	<0.001
Beijing	-20.45	82.61	2.91	4.55	-0.60	<0.001
Duolun	-27.38	88.48	2.87	5.41	-0.71	<0.001
Luancheng	-17.60	84.42	2.39	3.58	-0.61	<0.001
<i>δ¹⁸O (‰) Versus PBL Height (km)</i>						
New Haven	-4.88	-11.36	0.65	0.84	-0.64	<0.001
Borden	-3.81	-15.99	1.16	1.28	-0.35	0.002
Rosemount	-2.85	-14.28	0.93	1.49	-0.34	0.003
Beijing	0.16	-16.24	0.50	0.77	0.03	0.751
Duolun	-1.68	-16.70	0.83	1.57	-0.22	0.046
Luancheng	-0.39	-15.84	0.42	0.64	-0.10	0.360
<i>δD (‰) Versus PBL Height (km)</i>						
New Haven	-30.56	-81.86	4.30	5.58	-0.62	<0.001
Borden	-21.75	-118.04	8.18	9.00	-0.29	0.010
Rosemount	-14.50	-108.19	6.33	10.12	-0.26	0.025
Beijing	0.60	-120.47	3.70	5.69	0.02	0.871
Duolun	-12.09	-120.76	6.41	12.12	-0.20	0.063
Luancheng	-3.19	-117.59	3.57	5.34	-0.09	0.374

^aHere m = slope, b = intercept, sm = slope error, sb = intercept error, R = correlation coefficient, and P = statistical significant test. Bold values indicate statistical significance at the 98% confidence interval.

relationships with specific humidity at Beijing [Wen et al., 2010]. To remove the influence of evapotranspiration on d_v , the d of the surface water vapor flux was held at a constant equal to the initial surface layer d_v value. The results demonstrate that mixing and entrainment could produce increases in d_v from early morning to mid-afternoon in magnitude similar to that of the observed changes (Figure S2 in the auxiliary materials).

[37] We present two testable hypotheses for vertical profiles of d_v from the surface to the lower troposphere to explain our observations. (1) An increase in d_v with altitude could be unique to eastern North America caused by evaporation off the Great Lakes resulting in high d_v at altitude downwind, similar to Gat's lee-side convective model [Gat et al., 2003]. (2) Partial re-evaporation of raindrops below the cloud base increases d of the surrounding vapor [Lee and Fung, 2007]. This process could be common to most regions, but during the summer months, the Chinese monsoon has erased such a gradient in d_v because of enhanced vertical mixing and large downpours with little chance for raindrop evaporation during descent. We examined the d_v outside of the summer monsoon season to test this hypothesis and found no correlation with PBL height at either New Haven or Beijing; however, greater noise in the data during the drier non-summer months may hide any such signal.

[38] Turning our attention to plant transpiration, a common assumption has been that isotope ratios of plant transpiration equal those of xylem water. This is true for $\delta^{18}\text{O}$ and δD when averaged over days, or during short time-scales under steady state conditions, but not under nonsteady state conditions [e.g., Farquhar and Cernusak, 2005; Lai et al., 2006; Welp et al., 2008; Xiao et al., 2010]. The isotopic land surface model SiLSM [Xiao et al., 2010] provides support for the role of nonsteady state plant transpiration in the daytime increase in d_v . This model consists of a standard land surface sub-model for water and carbon dioxide exchange, a nonsteady state theory of leaf water isotopic composition, and a formulation of the kinetic fractionation at the canopy scale. The model has been tested against field observations of the $\delta^{18}\text{O}$ composition of evapotranspiration at Rosemount during a soybean year [Xiao et al., 2010] and at the Luancheng cropland [Xiao et al., 2012]. Here we have extended the model to the δD tracer with the inclusion of the appropriate fractionation factors. Model simulations for the Luancheng cropland were parameterized using field measurements of plant xylem water isotopes, averaging -6.3% , -53.5% and -3.3% for $\delta^{18}\text{O}$, δD and d respectively during the wheat phase and -7.0% , -59.5% and -3.5% respectively during the corn phase. Since corn and wheat have different leaf physiology and stomatal control, they have been parameterized differently in the model. The model results reveal a strong diurnal cycle in the d of transpiration (d_T) for both the corn and wheat growing periods that are more or less in phase with the diurnal composition of d_v observed at this site (Figure 7). Averaged over the entire growing season, the d_T was negative at night (-200 to -150%), increased rapidly after sunrise and peaked at 20 to 50% in mid-morning hours and remained high through the mid-afternoon. The model results are in agreement with recent observations in a forest showing the d of evapotranspiration peaked in mid-day [Wen et al., 2012]. The SiLSM-modeled d_T results show plant transpiration is a likely contributor to the diurnal variability in d_v .

[39] We do not have complete data on the forcing variables to run SiLSM for other sites. Sensitivity analysis suggests that ecosystems with a lower stomatal resistance should have more diurnally varying d_T (Figure 7). Perhaps this explains why the diurnal amplitude at the irrigated Luancheng crop site was lower than at the rainfed maize site

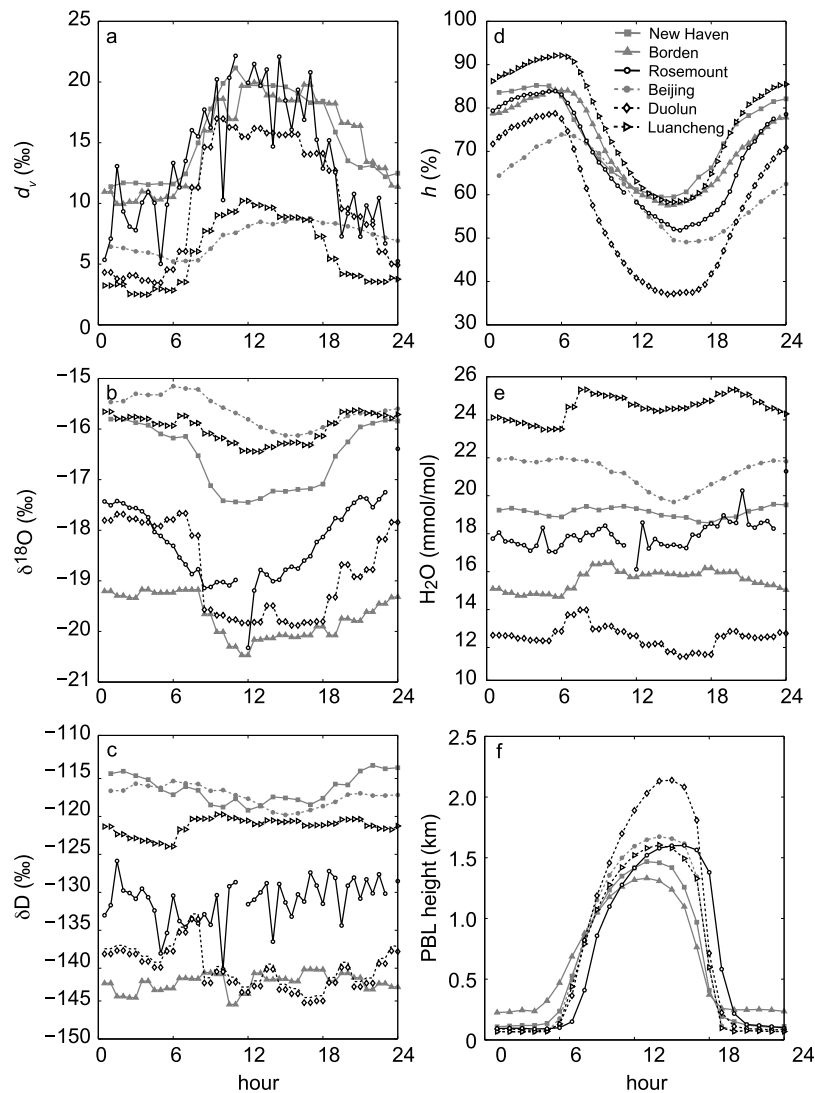


Figure 5. Mean diurnal cycles from June–August of (a) d of vapor, (b) $\delta^{18}\text{O}$ of vapor, (c) δD of vapor, (d) h relative to local air temperature, (e) water vapor mixing ratio, and (f) planetary boundary layer (PBL) height shown for each site.

in Rosemount and at the two natural ecosystems (Borden and Duolun).

[40] Finally, we discuss the potential role of surface evaporation from soils. It is possible that the daytime increase in d_v is partially driven by the diurnal pattern in the soil evaporation, a small flux of water, but which tends to have large d_v values. Soil evaporation is expected to be a minor component of evapotranspiration at all sites except Beijing during the summer. Field observations show that at times when LAI is greater than 2, evaporation is generally less than 10% of the total evapotranspiration flux to the atmosphere, based on lysimeters measuring soil evaporation and eddy covariance measuring total evapotranspiration flux [Lee *et al.*, 2007b; Griffis *et al.*, 2010]. Soil evaporation typically follows a diurnal pattern nearly identical to transpiration that peaks in mid-afternoon following incoming solar radiation making it difficult to separate from plant transpiration. The evaporation flux is also enhanced by the lower h during the daytime (Figure 5d). Using the observed isotope compositions of soil water at Luancheng, the d of soil evaporation varied in the

range of 160 to 210‰ through the diurnal cycle according to the Craig-Gordon model prediction in SiLSM. These large d values could be enough to contribute to d_v variability even by a relatively small portion of total evapotranspiration.

5. Conclusions

[41] The dominant feature that all sites shared was the mid-day increase in d_v with remarkably similar phases in the time progression. We predict that this diurnal pattern will be observed at many other locations as the number of d_v measurements increases. The fact that surface d_v in these continental settings varies so much diurnally and from day to day casts doubt on its application as a conservative tracer of oceanic moisture source region and conditions. For instance, day-to-day variability at New Haven and Borden Forest was correlated with local h , suggesting a contribution of evaporation from nearby large bodies of water at these sites. Therefore, the approaches previously used to interpret d of ice sheets and marine vapor are not directly transferable to

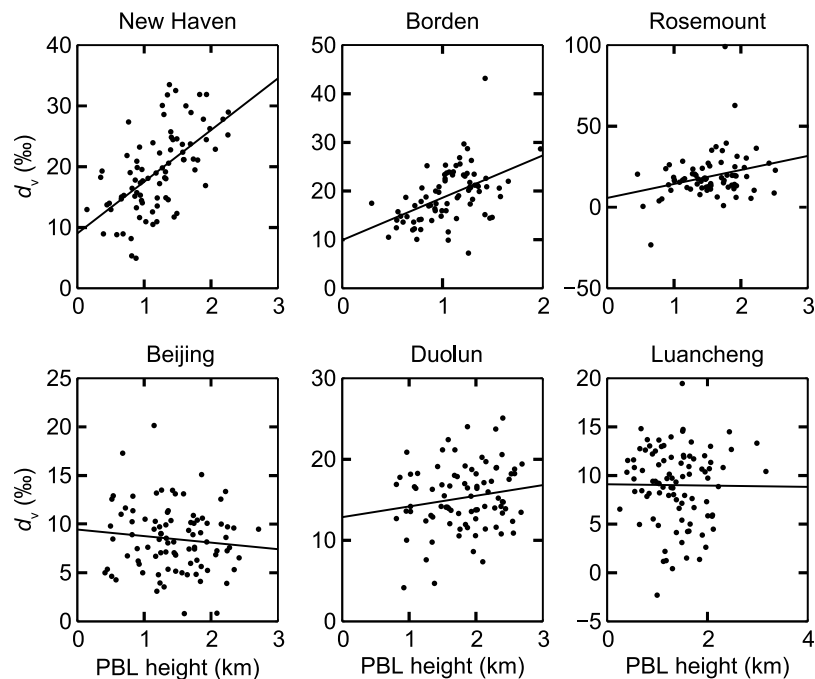


Figure 6. Afternoon (12:00–18:00 local time) mean d_v versus afternoon mean PBL height in the summer (June–August). Fit statistics are summarized in Table 2.

terrestrial d_v interpretation because of the influence of land processes.

[42] Comparing and contrasting measurements from multiple sites pointed to some differences in d_v controls among ecosystems and geographic settings. The stronger correlation of d_v with PBL height at the northeastern North American sites compared to the sites near Beijing, China suggests that the isotopic forcing of entrainment may not be the same in the two regions. Further work is needed to resolve the role of entrainment on hydrogen and oxygen isotopes of water vapor, and how they vary regionally due to large-scale moisture transport like the Asian monsoon and the influence of the Great Lakes. Our analysis yielded two hypotheses that could be tested by measuring vertical profiles of d_v from the surface through the lower troposphere in the study areas presented here.

[43] Simulations with the isotopic land surface model and large-eddy simulation model show that entrainment and plant transpiration can produce the observed diurnal variations, although it is difficult to separate their effects because their diurnal variability is tied to solar forcing, and they both have nearly identical timing. The relative contributions of entrainment versus evapotranspiration will likely vary with location and time of year. Comparing Beijing to the vegetated sites in China, we would predict the evapotranspiration influence is stronger than entrainment during summer in eastern China. Ultimately, measurements of the isotopic composition of the evapotranspiration flux [e.g., *Griffis et al.*, 2011a; *Wen et al.*, 2012] and detailed isotopic modeling of the surface atmosphere (for example with SiLSM) at individual sites will be necessary to quantify the relative roles of evapotranspiration and atmospheric mixing to time series of d_v . It is encouraging that the magnitude of the diurnal amplitude in d_v is large at sites of high transpiration fluxes. Features like this may make partitioning evapotranspiration

into evaporation and transpiration possible in the future. However, given the evidence of the role of entrainment, it may be that atmospheric d_v is better suited to partitioning at the regional scale than at the smaller ecosystem scale.

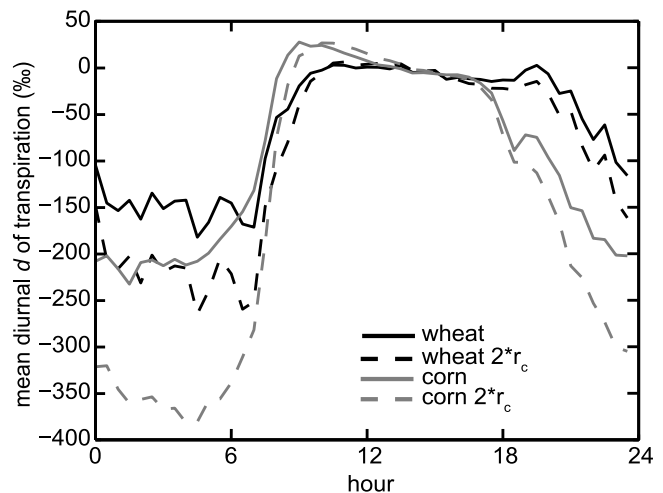


Figure 7. SiLSM model results of the mean diurnal cycle of d of transpiration (d_T) at Luancheng for the wheat (black solid) and corn (gray solid) phases during the 2008 growing season. In the mid-afternoon, d_T approaches the average d value of xylem water in the model, approximately -3.5‰ for both the wheat and corn phases. Also shown are the results of a sensitivity test where canopy resistance (r_c) was doubled (dotted lines). Higher canopy resistance results in a departure from steady state transpiration and larger diurnal amplitude in the isotopic forcing of transpiration.

[44] **Acknowledgments.** Portions of this study were supported by the Ministry of Science and Technology of China (grant 2010CB833501), the Ministry of Education of China (grant PCSIRT), the Strategic Program of Knowledge Innovation of the Chinese Academy of Sciences (grant KZCX2-EW-QN305), and the National Natural Science Foundation of China (grants 31100359, 31070408, and 30970517). Additional support was provided by the U. S. National Science Foundation (grants ATM-0914473 and ATM-0546476). We thank the Luancheng Agricultural Station of Chinese Ecosystem Research Network (CERN) and Duolun Grassland Station of Institute of Botany for providing the necessary infrastructure and Sandra Brown, Kyounghee Kim, Eduardo Santos, Shiuchun Zhang for assistance with the field experiments.

References

- Angert, A., J. E. Lee, and D. Yakir (2008), Seasonal variations in the isotopic composition of near-surface water vapour in the eastern Mediterranean, *Tellus, Ser. B*, 60(4), 674–684, doi:10.1111/j.1600-0889.2008.00357.x.
- Araguas-Araguas, L., K. Froehlich, and K. Rozanski (2000), Deuterium and oxygen-18 isotope composition of precipitation and atmospheric moisture, *Hydrol. Processes*, 14(8), 1341–1355.
- Bowen, G. J., and J. Revenaugh (2003), Interpolating the isotopic composition of modern meteoric precipitation, *Water Resour. Res.*, 39(10), 1299, doi:10.1029/2003WR002086.
- Clark, I. D., and P. Fritz (1997), *Environmental Isotopes in Hydrogeology*, CRC Press, Boca Raton, Fla.
- Craig, H. (1961), Isotopic variations in meteoric waters, *Science*, 133(346), 1702–1703.
- Cuffey, K. M., and F. Vimeux (2001), Covariation of carbon dioxide and temperature from the Vostok ice core after deuterium-excess correction, *Nature*, 412(6846), 523–527.
- Dansgaard, W. (1964), Stable isotopes in precipitation, *Tellus*, 16(4), 436–468.
- Darling, W. G., A. H. Bath, J. J. Gibson, and K. Rozanski (2006), Isotopes in water, in *Isotopes in Palaeoenvironmental Research*, edited by M. J. Leng, pp. 1–66, Springer, Amsterdam.
- Farquhar, G. D., and L. A. Cernusak (2005), On the isotopic composition of leaf water in the non-steady state, *Funct. Plant Biol.*, 32(4), 293–303, doi:10.1071/fp04232.
- Gat, J. R. (1996), Oxygen and hydrogen isotopes in the hydrologic cycle, *Annu. Rev. Earth Planet. Sci.*, 24, 225–262.
- Gat, J. R., C. J. Bowser, and C. Kendall (1994), The contribution of evaporation from the Great-Lakes to the continental atmosphere: Estimate based on stable isotope data, *Geophys. Res. Lett.*, 21(7), 557–560.
- Gat, J. R., B. Klein, Y. Kushnir, W. Roether, H. Wernli, R. Yam, and A. Shemesh (2003), Isotope composition of air moisture over the Mediterranean Sea: An index of the air-sea interaction pattern, *Tellus, Ser. B*, 55(5), 953–965.
- Griffis, T. J., et al. (2010), Determining the oxygen isotope composition of evapotranspiration using eddy covariance, *Boundary Layer Meteorol.*, 137(2), 307–326, doi:10.1007/s10546-010-9529-5.
- Griffis, T. J., N. Schultz, and X. Lee (2011a), Investigating the source, transport, and isotope composition of water in the atmospheric boundary layer, Abstract B24B-05 presented at 2011 Fall Meeting, AGU, San Francisco, Calif., 5–9 Dec.
- Griffis, T. J., X. Lee, J. M. Baker, K. Billmark, N. Schultz, M. Erickson, X. Zhang, J. Fassbinder, W. Xiao, and N. Hu (2011b), Oxygen isotope composition of evapotranspiration and its relation to C(4) photosynthetic discrimination, *J. Geophys. Res.*, 116, G01035, doi:10.1029/2010JG001514.
- He, H., and R. B. Smith (1999), Stable isotope composition of water vapor in the atmospheric boundary layer above the forests of New England, *J. Geophys. Res.*, 104(D9), 11,657–11,673.
- Henderson-Sellers, A. (2006), Improving land-surface parameterization schemes using stable water isotopes: Introducing the ‘iPILPS’ initiative, *Global Planet. Change*, 51(1–2), 3–24, doi:10.1016/j.gloplacha.2005.12.009.
- Intergovernmental Panel on Climate Change (2007), *Climate Change 2007: The Scientific Basis: Contribution of Working Group I to the Fourth Assessment Report of the Intergovernmental Panel on Climate Change*, edited by S. Solomon et al., 996 pp., Cambridge Univ. Press, New York.
- Jacob, H., and C. Sonntag (1991), An 8-year record of the seasonal variation of H-2 and O-18 in atmospheric water-vapor and precipitation at Heidelberg, Germany, *Tellus, Ser. B*, 43(3), 291–300.
- Johnson, D. G., K. W. Jucks, W. A. Traub, and K. V. Chance (2001), Isotopic composition of stratospheric water vapor: Measurements and photochemistry, *J. Geophys. Res.*, 106(D11), 12,211–12,217, doi:10.1029/2000JD900763.
- Johnson, L. R., Z. D. Sharp, J. Galewsky, M. Strong, A. D. Van Pelt, F. Dong, and D. Noone (2011), Hydrogen isotope correction for laser instrument measurement bias at low water vapor concentration using conventional isotope analyses: Application to measurements from Mauna Loa Observatory, Hawaii, *Rapid Commun. Mass Spectrom.*, 25(5), 608–616, doi:10.1002/rcm.4894.
- Jordan, N. S., R. M. Hoff, and J. T. Baumeister (2010), Validation of Goddard Earth Observing System-version 5 MERRA planetary boundary layer heights using CALIPSO, *J. Geophys. Res.*, 115, D24218, doi:10.1029/2009JD013777.
- Jouzel, J., L. Merlivat, and C. Lorius (1982), Deuterium excess in an East Antarctic ice core suggests higher relative-humidity at the oceanic surface during the last glacial maximum, *Nature*, 299(5885), 688–691.
- Kurita, N., N. Yoshida, G. Inoue, and E. A. Chayanova (2004), Modern isotope climatology of Russia: A first assessment, *J. Geophys. Res.*, 109, D03102, doi:10.1029/2003JD003404.
- Lai, C. T., and J. Ehleringer (2011), Deuterium excess reveals diurnal sources of water vapor in forest air, *Oecologia*, 165(1), 213–223, doi:10.1007/s00442-010-1721-2.
- Lai, C. T., J. R. Ehleringer, B. J. Bond, and K. T. U. Paw (2006), Contributions of evaporation, isotopic non-steady state transpiration and atmospheric mixing on the delta O-18 of water vapour in Pacific Northwest coniferous forests, *Plant Cell Environ.*, 29(1), 77–94.
- Lee, J.-E., and I. Fung (2007), “Amount effect” of water isotopes and quantitative analysis of post-condensation processes, *Hydrol. Processes*, 22(1), 1–8, doi:10.1002/hyp.6637.
- Lee, X., S. Sargent, R. Smith, and B. Tanner (2005), In situ measurement of the water vapor O-18/O-16 isotope ratio for atmospheric and ecological applications, *J. Atmos. Oceanic Technol.*, 22(5), 555–565.
- Lee, X., R. Smith, and J. Williams (2006), Water vapour O-18/O-16 isotope ratio in surface air in New England, USA, *Tellus, Ser. B*, 58(4), 293–304, doi:10.1111/j.1600-0889.2006.00191.x.
- Lee, J. E., I. Fung, D. J. DePaolo, and C. C. Henning (2007a), Analysis of the global distribution of water isotopes using the NCAR atmospheric general circulation model, *J. Geophys. Res.*, 112, D16306, doi:10.1029/2006JD007657.
- Lee, X., K. Kim, and R. Smith (2007b), Temporal variations of the ¹⁸O/¹⁶O signal of the whole-canopy transpiration in a temperate forest, *Global Biogeochem. Cycles*, 21, GB3013, doi:10.1029/2006GB002871.
- Lee, X., J. Huang, and E. G. Patton (2012), A large-eddy simulation study of water vapour and carbon dioxide isotopes in the atmospheric boundary layer, *Boundary Layer Meteorol.*, in press.
- Masson-Delmotte, V., J. Jouzel, A. Landais, M. Stievenard, S. J. Johnsen, J. W. C. White, M. Werner, A. Sveinbjornsdottir, and K. Fuhrer (2005), GRIP deuterium excess reveals rapid and orbital-scale changes in Greenland moisture origin, *Science*, 309(5731), 118–121, doi:10.1126/science.1108575.
- Medeiros, B., A. Hall, and B. Stevens (2005), What controls the mean depth of the PBL?, *J. Clim.*, 18(16), 3157–3172.
- Merlivat, L., and J. Jouzel (1979), Global climatic interpretation of the deuterium-oxygen-18 relationship for precipitation, *J. Geophys. Res.*, 84(C8), 5029–5033.
- Mitchell, J. F. B. (1989), The greenhouse-effect and climate change, *Rev. Geophys.*, 27(1), 115–139, doi:10.1029/RG027i001p00115.
- Pfahl, S., and H. Wernli (2008), Air parcel trajectory analysis of stable isotopes in water vapor in the eastern Mediterranean, *J. Geophys. Res.*, 113, D20104, doi:10.1029/2008JD009839.
- Risi, C., S. Bony, F. Vimeux, and J. Jouzel (2010), Water-stable isotopes in the LMDZ4 general circulation model: Model evaluation for present-day and past climates and applications to climatic interpretations of tropical isotopic records, *J. Geophys. Res.*, 115, D12118, doi:10.1029/2009JD013255.
- Rozanski, K., L. Araguás-Araguás, and R. Gonfiantini (1993), Isotopic patterns in modern global precipitation, in *Climate Change in Continental Isotopic Records*, *Geophys. Monogr. Ser.*, vol. 78, edited by P. K. Swart et al., pp. 1–36, AGU, Washington, D. C., doi:10.1029/GM078p0001.
- Santer, B. D., et al. (2007), Identification of human-induced changes in atmospheric moisture content, *Proc. Natl. Acad. Sci. U. S. A.*, 104(39), 15,248–15,253, doi:10.1073/pnas.0702872104.
- Santos, E., C. Wagner-Riddle, X. Lee, J. Warland, S. Brown, R. Staebler, P. Bartlett, and K. Kim (2011), Use of the isotope flux ratio approach to investigate the C¹⁸O¹⁶O and ¹³CO₂ exchange near the floor of a temperate deciduous forest, *Biogeosci. Discuss.*, 8, 7671–7712.
- Schmidt, M., K. Maseyk, C. Lett, P. Biron, P. Richard, T. Bariac, and U. Seibt (2010), Concentration effects on laser-based ^δ18O and ^δ2H measurements and implications for the calibration of vapour measurements with liquid standards, *Rapid Commun. Mass Spectrom.*, 24(24), 3553–3561, doi:10.1002/rcm.4813.

- Schneider, M., and F. Hase (2011), Optimal estimation of tropospheric H₂O and delta D with IASI/METOP, *Atmos. Chem. Phys.*, *11*(21), 11,207–11,220.
- Steffensen, J. P., et al. (2008), High-resolution Greenland ice core data show abrupt climate change happens in few years, *Science*, *321*(5889), 680–684, doi:10.1126/science.1157707.
- Stewart, M. K. (1975), Stable isotope fractionation due to evaporation and isotopic exchange of falling waterdrops: Applications to atmospheric processes and evaporation of lakes, *J. Geophys. Res.*, *80*(9), 1133–1146, doi:10.1029/JC080i009p01133.
- Trenberth, K. E., L. Smith, T. Qian, A. Dai, and J. Fasullo (2007), Estimates of the global water budget and its annual cycle using observational and model data, *J. Hydrometeorol.*, *8*(4), 758–769, doi:10.1175/JHM600.1.
- Uemura, R., Y. Matsui, K. Yoshimura, H. Motoyama, and N. Yoshida (2008), Evidence of deuterium excess in water vapor as an indicator of ocean surface conditions, *J. Geophys. Res.*, *113*, D19114, doi:10.1029/2008JD010209.
- Wang, L., K. K. Caylor, and D. Dragoni (2009), On the calibration of continuous, high-precision $\delta^{18}\text{O}$ and $\delta^2\text{H}$ measurements using an off-axis integrated cavity output spectrometer, *Rapid Commun. Mass Spectrom.*, *23*(4), 530–536, doi:10.1002/rcm.3905.
- Webster, C. R., and A. J. Heymsfield (2003), Water isotope ratios D/H, $^{18}\text{O}/^{16}\text{O}$, $^{17}\text{O}/^{16}\text{O}$ in and out of clouds map dehydration pathways, *Science*, *302*, 1742–1745, doi:10.1126/science.1089496.
- Welp, L. R., X. Lee, K. Kim, T. J. Griffis, K. A. Billmark, and J. M. Baker (2008), $\delta^{18}\text{O}$ of water vapour, evapotranspiration and the sites of leaf water evaporation in a soybean canopy, *Plant Cell Environ.*, *31*(9), 1214–1228, doi:10.1111/j.1365-3040.2008.01826.x.
- Wen, X.-F., X.-M. Sun, S.-C. Zhang, G.-R. Yu, S. D. Sargent, and X. Lee (2008), Continuous measurement of water vapor D/H and O-18/O-16 isotope ratios in the atmosphere, *J. Hydrol.*, *349*(3–4), 489–500, doi:10.1016/j.jhydrol.2007.11.021.
- Wen, X.-F., S.-C. Zhang, X.-M. Sun, G.-R. Yu, and X. Lee (2010), Water vapor and precipitation isotope ratios in Beijing, China, *J. Geophys. Res.*, *115*, D01103, doi:10.1029/2009JD012408.
- Wen, X.-F., X. Lee, X.-M. Sun, J.-L. Wang, Z.-M. Hu, S.-G. Li, and G.-R. Yu (2011), Dew water isotopic ratios and their relationships to ecosystem water pools and fluxes in a cropland and a grassland in China, *Oecologia*, *168*, 549–561, doi:10.1007/s00442-011-2091-0.
- Wen, X. F., Y. Tang, X. Sun, and X. Lee (2012), Temporal variations of d-excess in water vapor above a subtropical conifer plantation in southeastern China, paper presented at the Conference on Agricultural and Forest Meteorology, Am. Meteorol. Soc., Boston, Mass.
- Werner, M., P. M. Langebroek, T. Carlsen, M. Herold, and G. Lohmann (2011), Stable water isotopes in the ECHAM5 general circulation model: Toward high-resolution isotope modeling on a global scale, *J. Geophys. Res.*, *116*, D15109, doi:10.1029/2011JD015681.
- Willett, K. M., N. P. Gillett, P. D. Jones, and P. W. Thorne (2007), Attribution of observed surface humidity changes to human influence, *Nature*, *449*(7163), 710–712, doi:10.1038/nature06207.
- Worden, J., et al. (2006), Tropospheric Emission Spectrometer observations of the tropospheric HDO/H₂O ratio: Estimation approach and characterization, *J. Geophys. Res.*, *111*, D16309, doi:10.1029/2005JD006606.
- Worden, J., D. Noone, and K. Bowman (2007), Importance of rain evaporation and continental convection in the tropical water cycle, *Nature*, *445*(7127), 528–532, doi:10.1038/nature05508.
- Xia, J. Y., S. L. Niu, and S. Q. Wan (2009), Response of ecosystem carbon exchange to warming and nitrogen addition during two hydrologically contrasting growing seasons in a temperate steppe, *Global Change Biol.*, *15*(6), 1544–1556, doi:10.1111/j.1365-2486.2008.01807.x.
- Xiao, W., X. Lee, T. J. Griffis, K. Kim, L. R. Welp, and Q. Yu (2010), A modeling investigation of canopy-air oxygen isotopic exchange of water vapor and carbon dioxide in a soybean field, *J. Geophys. Res.*, *115*, G01004, doi:10.1029/2009JG001163.
- Xiao, W., X. Lee, X. Wen, X. Sun, and S. Zhang (2012), Modeling biophysical controls on canopy foliage water ^{18}O enrichment in wheat and corn, *Global Change Biol.*, *18*(5), 1769–1780, doi:10.1111/j.1365-2486.2012.02648.x.
- Yoshimura, K., M. Kanamitsu, D. Noone, and T. Oki (2008), Historical isotope simulation using reanalysis atmospheric data, *J. Geophys. Res.*, *113*, D19108, doi:10.1029/2008JD010074.
- Zhang, W. L., S. P. Chen, J. Chen, L. Wei, X. G. Han, and G. H. Lin (2007), Biophysical regulations of carbon fluxes of a steppe and a cultivated cropland in semiarid Inner Mongolia, *Agric. For. Meteorol.*, *146*(3–4), 216–229, doi:10.1016/j.agrformet.2007.06.002.
- Zhang, S. C., X. M. Sun, J. L. Wang, G. R. Yu, and X. F. Wen (2011), Short-term variations of vapor isotope ratios reveal the influence of atmospheric processes, *J. Geogr. Sci.*, *21*(3), 401–416, doi:10.1007/s11442-011-0853-6.
- Zielinski, G. A., and B. D. Keim (2003), *New England Weather, New England Climate*, Univ. Press of N. Engl., Lebanon, N. H.